First System for Interactive Position Planning of Implant Components

Michel Waringo, Philipp Stolka and Dominik Henrich

AG Eingebettete Systeme und Robotik (RESY)
Fachbereich Informatik, Gebäude 48
Universität Kaiserslautern, D-67653 Kaiserslautern
{p_stolka, henrich}@informatik.uni-kl.de,
http://resy.informatik.uni-kl.de/

Abstract. One of the steps during the implantation of hearing aids and cochlea implants is the creation of a shallow implant bed in the thin skull bone. Correct placement of the implant is paramount but difficult to achieve preoperatively. The profile of the calotte, which can be determined through e.g. 3D imaging, is important for this task. Additionally, in a robot-based surgical operation, the final position and orientation of the implant must be known before milling starts to ensure optimal fitting. We present an algorithm which allows semi-automatic determination of this optimal placement through both the planning system and the surgeon. The computer supports the surgeons with his speed and accuracy, while the robot aids in the precise execution.

1 Motivation

Case numbers for hearing loss are rising steadily. There are several kinds of hearing loss which can be handled with different types of hearing aids. Implantable hearing aids help with defective auditory canals. The ossicles are excited mechanically[1]. Cochlea implants directly stimulate the acoustic nerve in the cochlea, bypassing the sensitive hairs situated there[2].

During actual implantation of the hearing aid, the surgeon excavates an implant bed in the thin skull bone for one of the components (the amplifier). This milling procedure takes about a quarter to half an hour, requires maximum concentration of the surgeon and is thus physically exhausting. The bone often has to be resected up to the border of the dura mater, resulting in complications near the end of the process when the milling head tears through the dura.

Robotic milling, however, has several advantages over the conventional method:

- A robot needs no rest; precision stays the same over extended periods of time.
- Tearing of the dura during manual milling can be avoided.
- Furthermore, a high and reproducible process quality can be guaranteed.

[1] We differentiate fully implantable hearing aids (e.g. TICA by Implex) and partly implantable ones (e.g. Vibrant Soundbridge by Med-El/Symphonix).

[2] Examples are the Tempo+ by Med-El and the Nucleus by Cochlear.

Positioning of the implant in the bone usually occurs before and during the operation and is based on the surgeon's experience. Robot-based milling, however, requires complete preoperative planning, since intraoperative changes are costly in terms of time and risk. This calls for optimal planning procedures. Automation of surgical interventions allows to let this positioning be performed by the computer.

This work describes the robot-based RONAF system for implantation planning and milling in the skull [Henrich02], which for the first time performs this position optimization, co-operating with the surgeon.

First, we give a short overview over existing planning methods in section 2. Then, we describe the preparation of the optimization (section 3) and its execution (section 4). Finally, experimental validation through a comparison with manual optimization is described in section 5.

2. State of the Art

We present a short overview of existing planning systems in computer- and robot-assisted surgery as well as optimization procedures that are suited for use in such systems.

Planning of position and orientation (only called *position* from now on) of milling volumes is an important step in computer- as well as robot-assisted surgical interventions. One possibility is direct registration of the patient with a coordinate system that is associated with the milling volume and the robot, e.g. through manual guidance (force following) of the robot. Basically, three non-collinear points on the patient suffice for intraoperative position definition. The robot should be usable as transparently as possible through appropriate control algorithms [Stolka03]. While this procedure is easy to implement, the user may have problems with the additional abstraction from the milling volume to the representing points during force following.

An image-based variant is to display a three-dimensional template of the milling volume within the planning data (e.g. slice or biplanar images) and to position it manually. This is especially important in complex or mechanically loaded environments (e.g. the mastoid or the femur). Planning of the implantation of e.g. hearing aids can be done this way [Dammann01]. The mastoid is being measured through spiral CT images and converted into a triangle mesh. Both the mastoid and an implant geometry are then displayed in the virtual reality system REALAX, allowing a preoperative implantability check. This demonstrates that current computer systems exhibit sufficient performance for such simulations.

Implantation of hip endoprosthesises with the ROBO-/ORTHODOC system is done in a similar way [Davies00]. Position planning of the femur endoprosthesis is performed by displaying together a CT-based three-dimensional model of the bone with an implant template, which can be manipulated manually. Then, milling paths are generated to be followed by a SCARA robot, which performed the first orthopedic intervention on a human in 1992.

Radermacher et al. have developed the CRIGOS-System for robot-based orthopedic interventions, e.g. hip implantation [Brandt02]. Position planning is done by displaying template geometries into a three-dimensional reconstruction of the bone from biplanar image data; this way, avoiding CT imaging.

Concerning optimization algorithms, we differentiate between several types of algorithms, depending on the problem at hand [Hamacher03], [Hocks95]:

- Linear problems can be solved with standard algorithms like Simplex (first choice for smaller problems with less than 1000 variables) or Karmarkar (best for problems larger than 1000 variables).
- Non-linear problems can be solved through algorithms from one of the following subclasses: Algorithms that optimize the single variables successively and those that optimize all variables simultaneously. Among the first type, we find discrete optimization and gradient descent algorithms, while the latter include Simulated Annealing and Downhill Simplex.
- One ocurence of nonlinear problems is the matching of general geometries (*registration*). One can use matching algorithms like the Closest Point Algorithm or the stochastic variant Iterative Closest Point.

The investigated task is to automatically optimize the position of an implant geometry (the *milling geometry*) in relation to the skull profiles (the *milling material*). Optimization criteria are geometric relations between the respective contours (cf. section 3). Because of the irregular shape of the bone, these cannot be stated in linear form, which is why we do not use linear optimization. Instead, we settled for a discrete optimization procedure which matches points of the milling geometry as good as possible with their respective counterparts on the milling material. Planning data is based on slice imaging because of the complex structures in the intervention region which cannot be reconstructed from e.g. biplanar data.

3. Preparatory Steps for Optimization

For the optimization process, we need a description of the milling volume as a three-dimensional triangle mesh as well as image data of the milling material, e.g. from CT slice images.

From the description of the milling material, we generate two 2.5-dimensional height arrays D_{KU} (lower profile) and D_{KO} (upper profile) which allow interpolating read access to achieve higher lateral precision of the height information. Each (x, y) position thus holds only two z indices for the bone; therefore information is lost when the bone undercuts (cf. Figure 2). Hence, the presented procedure is specialized on flat bone structures.

From the triangle description D_{stl} of the milling volume, however, we generate a rastered voxel representation D_V, starting from which we calculate three sets of optimization points serving as representatives of the volume for the optimization:

- The set O_{UA} of points at the outer ridge of the lower contour. These points have to stay at least one millimeter above the lower bone profile after optimization.
- The set O_{UI} of points which are on the lower contour as well, but which sit five millimeters nearer to the center. After optimization, these points need to lie above the lower bone profile.
- The set O_O of optimization points at the upper ridge of the milling volume. These serve as hints for the fit of the upper profile of both milling volume and milling material.

In Figure 1, the regions where the two sets of lower optimization points can be found are marked on the main module of the TICA implant. For O_{UA} and O_{UI} we single out the locations with the highest curvature changes of the lower and upper contour of the milling volume. These locations sit near the edge of the milling volume and belong to the optimization points. For volumes with only slightly curved edges, one finds the locations where the curvature begins, while for volumes with sharply defined edges one finds exactly those edges.

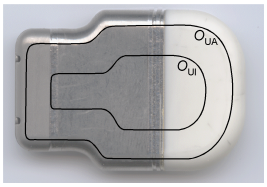

Figure 1: Lower optimization point sets O_{UI}, O_{UA} marked on the lower contour of the TICA implant

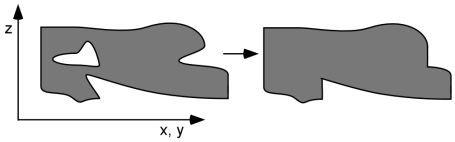

Figure 2: Original, undercutting bone geometry (left); representation used by the program (right) (grey: image points defined as bone)

For the optimization, the sets of optimization points given in a local coordinate system are transformed into the coordinates of the milling material and the resulting optimization value is calculated. The same transformation is applied to all points, i.e. the milling volume is treated as a rigid body.

The optimization problem is formulated as the minimization of the optimization value. This is achieved through minimization of the distance between the upper contours of both the milling volume and milling material, expressed as mean square error (*MSE*) distance v_{opt} between points from O_O and their projections onto D_{KOI} along the *z* axis. The smaller this value, the better aligned are the upper profiles.

An optimization constraint is that the milling volume may not protrude below the lower milling material profile since the implant might lose fit later. Directly at the edge of the milling volume, remaining bone thickness must be at least one millimeter, and some bone support must still be in place five millimeters further to the center of the milling volume. This guarantees a "balcony" of bone below the implant. However, because of the dura mater's elasticity and because the bone still offers enough support even through only a few contact points, we can allow that up to a few percent (in the experiments we set this to 10%) of the optimization points violate this constraint. The optimization constraint value v_{cond} is calculated by counting points from O_{UA} or O_{UI} that lie below D_{KUI} along the *z* axis.

4. Optimization Process

Position optimization is done cooperatively. The user, giving an initial position for the milling volume, and the program, fine-tuning this position, take turns. When the user agrees with the position he terminates this cooperative process.

For the automatic optimization steps, the program is restrained to a small region around the position proposed by the user. The knowledge and experience of the user could not be exploited if the program searched for a global optimum over the whole represented skull area. Thus, the proposed scheme does not search globally, but seeks out a local optimum

in the vicinity of the starting position[1]. The user can selectively disable subsets of the six degrees of freedom, gaining even greater control over the result of the cooperative optimization.

For the automatic optimization, we use a discrete optimization scheme. The degrees of freedom are rotations $\mathbf{r} \in \Re^3$ about the *x*, *y*, and *z* axes as well as translations $\mathbf{s} \in \Re^3$ along the *x*, *y* and *z* axes. Of these, only one is modified at a time. Input for the algorithm are the initial values for the rotations $\mathbf{r}_0 \in \Re^3$ and the translations $\mathbf{s}_0 \in \Re^3$ which are both determined through the user's initial position.

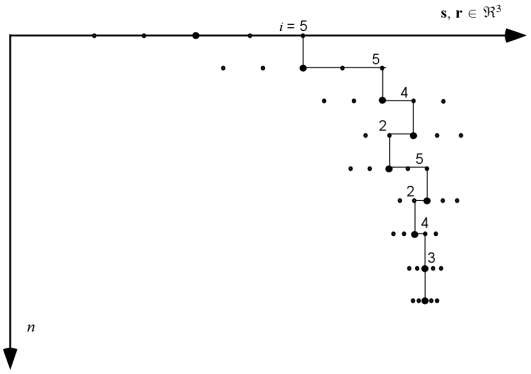

Figure 3: Optimization of one variable. On the x axis, we find the value of the current degree of freedom plotted against the iteration step n on the y axis. The marked point indicates the chosen value from the neighboring i_{max} ones.

Furthermore, there exist boundaries for the translation and rotation values to be determined during optimization. This enforces a resulting position in the vicinity of the initial position given by the user. The three translations have an initial motion range $\mathbf{f}_S \in \Re^3$ of 20 millimeters in each direction to search for better positions. The positions to be checked are distributed equidistantly around the current position **s**; we check $i_{max} = 21$ different positions. The interval length defining the position range is being reduced with the factor $l = 0.95$ after each iteration, guaranteeing convergence of the algorithm (cf. Figure 3). This applies analogously for rotations. Their initial range $\mathbf{f}_R \in \Re^3$ of 1 rad (180°) in each direction is being reduced as well.

5. Experimental Validation

For experimental validation, we test the performance of the proposed automatic optimization procedure in relation to the user's. In order to do so, we create an artificial planning situation in which both have to optimize the position of a hearing aid component in the skull bone.

[1] Since we employ a multidimensional discrete optimization procedure, an exhaustive neighborhood search would result in combinatorial explosion. Therefore, we simplify to one dimension and thus search for "one-dimensional local optima".

As a visual aid, a graphical preview of the milling volume, the optimization points and the milling material is presented (cf. Figure 4). The milling volume position can be modified through sliders. The optimization and constraint values v_{opt} and v_{cond} are calculated and displayed concurrently.

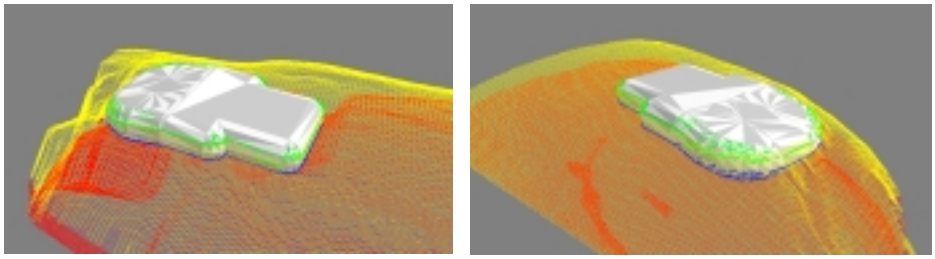

Figure 4: Two views of the TICA implant with part of the image data, in optimized position

Three initial positions of the milling volume are set randomly. From this position, both the user and the program are allowed to perform optimization. The values of the optimization values are not shown to the user to preserve the original planning situation with only visual hints. As soon as the user wishes to end optimization, the values are displayed and saved. Then the program performs the optimization, for which the resulting values are saved. The durations of the optimizations are recorded for both the program and the user. Finally, the milling volume and the milling material are exchanged systematically and this process is repeated.

We used three implants geometries: Combi40+ (by Med-El), Vibrant Soundbridge (by Med-El/Symphonix) and TICA (by Implex). The image data sets used were segments of CT data of a real skull (*Os temporalis*, resolution 0.4×0.4×1.1mm³) and a synthetic geometry (a layer of thickness 4.4mm). The experiment was carried out with two test persons which were allowed to learn manipulation of the positions before the experiment.

The results of the experiments with the real skull geometry follow. The results with the synthetic geometry were similar; however, for some experiments, the automatic optimization procedure needed two steps to reach a good enough position. This was caused by a position too high above the surface – the algorithm converged too fast to reach the surface (reduction of the motion interval length *l*; cf. section 4).

Implant	t_{total} [min:sec]		v_{opt} [mm²]		v_{cond} [%]	
	User	**Program**	**User**	**Program**	**User**	**Program**
Combi40+	0:50.65	0:04.99	0,61	0,34	0	0
	0:55.57	0:05.05	28,68	7,55	0	0
	0:12.03	0:08.28	23,84	0,21	0	0
Soundbridge	0:43.35	0:05.03	15,21	0,38	0	0
	1:02.28	0:10.20	10,33	0,38	0	0
	0:34.05	0:05.50	1,21	0,47	0	0
TICA	0:56.46	0:08.90	21,91	1,78	43,77	4,13
	1:05.12	0:06.22	15,19	0,97	28,06	0,14
	0:53.40	0:05.87	2,94	2,01	2,99	4,90

Table 1. Comparison of duration t, optimization value v_{opt} and constraint violation v_{cond} of manual and automatic position optimization of three implants in the temporal bone

The results confirm the expectation that the automatic optimization procedure is superior compared with the user. The duration t of the optimization runs is very small on the system used (five to ten seconds, excluding preparation), the optimization value v_{opt} is always smaller than the user's (with a factor of 1.5 to 40), and finally, the constraint ($v_{cond} < 5\%$) is never violated, in contrast to manual optimization.

Furthermore, the optimization value is calculated considering only the generated optimization points. Hence, this value does not necessarily reflect the actual quality of the position as the milling volume might infringe on the lower milling material profile between those points.

6. Conclusion

The experiments show that automatic position optimization is superior to the manual procedure, at least insofar as the criteria used in this work are relevant.

The proposed procedure is applicable only to plane milling material structures by principle. This restriction is based in the 2.5-dimensional representation of lower and upper profile of the milling material. Furthermore, the material must be non-undercutting.

The curvature-based procedure to generate optimization points is suited for the implant geometries used, but results in inferior point sets for highly rounded geometries – an extreme case would be a sphere. Without clearly defined edges, there are no clear curvature changes that could be used for optimization points. However, a human user would have problems with the position planning for such geometries as well.

7. Future Work

As an extension for the proposed scheme we will use 3D ultrasound imaging as an option or an alternative in order to enhance the axial precision of the image data for at least an order of magnitude [Federspil03]. This would directly yield the two bone profiles instead of necessitating an error-prone reconstruction. This is relevant since for the used robot system, the achievable accuracy is higher along the z axis, allowing less conservative position planning [Stolka02].

Of major relevance for the application are the used optimization criteria. Until now, we only considered the mean distance and protrusion below the milling material. Other criteria for our application include the orientation and the distance of the implant component relative to the mastoid as well as to the outer ear; those will be integrated in the next steps.

Acknowledgement

This work is part of the project "Robot-based Navigation for Milling at the Lateral Skull Base (RONAF)" which is part of the special research cluster "Medical Navigation and Robotics (SPP 1124)" and is funded by the Deutsche Forschungsgemeinschaft (DFG).

References

[Brandt02] G. Brandt, K. Radermacher, A. Zimolong, G. Rau, P. Merloz, T.V.S. Klos, J. Robb, H.W. Staudte: *„CRIGOS – Entwicklung eines Kompaktrobotersystems für die bildgeführte orthopädische Chirurgie“*. In: Orthopädie 2000 – 29:645-649, Springer-Verlag. http://www.hia.rwth-aachen.de/research/cht/Crigos1.html. 2002

[Dammann01] F. Dammann, A. Bode, E. Schwaderer, M. Schaich, M. Heuschmid, M. M. Maassen: *„Computer-aided Surgical Planning for Implantation of Hearing Aids Based on CT Data in a VR environment“*. In: Radiographics, Volume 21 – Number 21: 183-190, 2001

[Davies00] B. L. Davies: „*A review of robotics in surgery*“. In: Proc Instn Mech Engers Vol 214 Part H, 2000

[Federspil03] Federspil, Ph. A.; Tretbar, S.H.; Geisthoff, U.; Plinkert, B.; Plinkert P.K.: „*Ultrasound based navigation of robotic drilling at the lateral skull base*“. In: H.E. Lemke, K. Inamura, K. Diu, M.W. Vannier, A.G. Farman and J.H.C. Reiber (Eds.): CARS 2003 - Computer Assisted Radiology and Surgery. Elsevier Science BV, pp. 1358. 2003

[Hamacher00] H. W. Hamacher, Kathrin Klamroth: „*Lineare und Netzwerk-Optimierung – ein bilinguales Lehrbuch*“, Vieweg, Teaching Material. Vieweg, Mathematics International. ISBN 3-528-03155-7

[Henrich02] Henrich, D.; Plinkert, P.K.; Federspil, Ph. A.; Plinkert, B.: „*Robotergestütztes Fräsen an der lateralen Schädelbasis: Kraft-basierte lokale Navigation bei der Implantatbettanlage*“. In: VDI-Bericht 1679 – Tagungshandbuch zur Robotik 2002, Ludwigsburg. 2002

[Hocks95] M. Hocks: „*Innere-Punkte-Methoden und automatische Ergebnisverifikation in der Linearen Optimierung*“, Dissertation, Fakultät der Mathematik der Universität Karlsruhe, Berlin, 1985. Internet: www.ubka.uni-karlsruhe.de/vvv/1995/mathematik/1/1.ps

[Stolka02] Stolka, Ph.: „*Robotergestützte Navigation zum Fräsen an der lateralen Schädelbasis (RONAF): Auswertung von Kraftsensordaten*“, Diploma Thesis. Universität Kaiserslautern, Fachbereich Informatik, AG Robotik und Eingebettete Systeme (RESY). 2002

[Stolka03] Stolka, Ph.: *„A Hybrid Force-Following Controller for Multi-Scale Motions“*. In: CURAC 2003, 7th International IFAC Symposium on Robot Control, Wrocław/Polen. 2003